Coupling the Higgs mode and ferromagnetic resonance in spin-split superconductors with Rashba spin-orbit coupling

Yao Lu [1,2] Risto Ojajärvi,[1] P. Virtanen,[1] M. A. Silaev,[1,3] and Tero T. Heikkilä [1]

[1]*Department of Physics and Nanoscience Center, University of Jyväskylä, P.O. Box 35 (YFL), FI-40014 University of Jyväskylä, Finland*
[2]*Centro de Física de Materiales (CFM-MPC), Centro Mixto CSIC-UPV/EHU, Manuel de Lardizabal 5, E-20018 San Sebastián, Spain*
[3]*Computational Physics Laboratory, Physics Unit, Faculty of Engineering and Natural Sciences, Tampere University,*
P.O. Box 692, Tampere, Finland

We show that the Higgs mode of superconductors can couple with spin dynamics in the presence of a static spin-splitting field and Rashba spin-orbit coupling. The Higgs-spin coupling dramatically modifies the spin susceptibility near the superconducting critical temperature and consequently enhances the spin pumping effect in a ferromagnetic insulator/superconductor bilayer system. We show that this effect can be detected by measuring the magnon transmission rate and the magnon-induced voltage generated by the inverse spin Hall effect.

I. INTRODUCTION

Superconductors (SCs) with broken $U(1)$ symmetry host two kinds of collective modes associated with the order parameter fluctuations: the phase mode and the amplitude mode. Coupled to a dynamical gauge field, the phase mode is lifted up to the plasma frequency [1] due to the Anderson-Higgs mechanism [2,3]. The other collective mode in SC is the amplitude mode [4,5] with an energy gap of 2Δ, called the Higgs mode by analogy with the Higgs boson [3] in particle physics. It was commonly believed that unlike the phase mode the Higgs mode usually does not couple linearly to any experimental probe. That is why in earlier experiments, the Higgs mode was only observed in charge-density-wave (CDW) coexisting systems [6–11]. With the advance of terahertz spectroscopy technique [12] it became possible to investigate the Higgs mode through the nonlinear light-Higgs coupling [13–18]. In these experiments, the perturbation of the order parameter is proportional to the square of the external electromagnetic field $\delta\Delta \propto E^2$, so very strong laser pulses are required.

Recently, it has been shown that in the presence of a supercurrent the Higgs resonance can actually contribute to the total admittance Y_Ω (Ω denotes the frequency) due to the linear coupling of the Higgs mode and the external electromagnetic field [19–23]. This can be understood from a symmetry argument. Suppose the external electric field is linearly polarized in the x direction $E = \hat{x}E_x e^{i\Omega t}$. The linear coupling of the Higgs mode and the external field is represented by the susceptibility $\chi_{\Delta E} = -\frac{\partial^2 S}{\partial \Delta \partial E}$ obtained from the action S describing the electron system containing the pair potential field Δ. Without a supercurrent, the system preserves the inversion symmetry ($\hat{I}$) and the mirror symmetry in the x direction ($\hat{M}_x$). On the other hand $\chi_{\Delta E}$ is odd under both these operations because E changes sign under $\hat{I}$ and $\hat{M}_x$ whereas

Δ remains the same. Therefore $\chi_{\Delta E}$ has to vanish. In the presence of a supercurrent, the inversion symmetry and the mirror symmetry are both broken and there is no restriction for $\chi_{\Delta E_x}$ from these symmetries, so $\chi_{\Delta E}$ can be nonzero. This symmetry argument also explains why the Higgs mode does not couple with an external field in the direction perpendicular to the supercurrent.

Now a natural question arises: without a supercurrent does the Higgs mode couple linearly with other external probes, such as spin exchange fields? As we show in this paper, it does. The above discussion indicates that the decoupling of the Higgs mode is protected by certain symmetries. In order to couple the Higgs mode to an external field one needs to break these symmetries. Here we show how it happens in a ferromagnetic insulator (FI)/superconductor (SC) bilayer system (Fig. 1). Magnons with momentum $\boldsymbol{q}$ and frequency Ω in the FI can be injected into the SC in a process known as spin pumping [24–30]. We predict that the Higgs mode in the SC couples linearly with the magnon mode in the FI in the presence of Rashba spin-orbit coupling and the magnetic proximity effect into the SC. In this system the symmetries protecting Higgs-spin decoupling are broken: in particular, the (spin) rotation symmetry and the time-reversal symmetry. Near the critical temperature, superconductivity is suppressed and Δ_0 becomes comparable with the magnon frequency Ω. When the magnon frequency matches the Higgs frequency $\Omega_M = 2\Delta_0$, the Higgs mode is activated and the magnon absorption is hugely enhanced which can be detected through the inverse spin Hall effect (iSHE) [31–33]. This effect can possibly explain the voltage peak observed in the experiment [34].

We consider a SC/FI bilayer in which the FI and the SC are coupled via the exchange interaction as shown in Fig. 1. For simplicity, we assume that the thickness d of the SC film is much smaller than the spin relaxation length and the coherence length so that we consider it as a two-dimensional
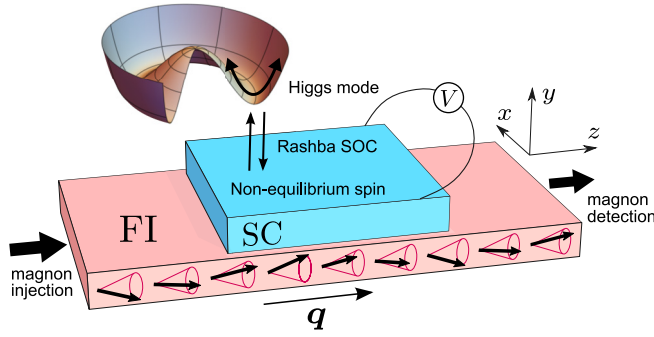
FIG. 1. System under consideration. A superconductor thin film is placed on the top of a FI with in-plane magnetization. The SC and FI are coupled via spin exchange interaction. The magnon in FI can be injected into SC in a process known as the spin pumping effect. For magnon frequency $\Omega = 2\Delta_0$ the SC Higgs mode greatly increases the spin pumping.

system. The magnetization of the FI can be written as $\boldsymbol{m} = \boldsymbol{m}_0 + \boldsymbol{m}_\Omega$, where $\boldsymbol{m}_0$ is the static magnetization polarized in the z direction and $\boldsymbol{m}_\Omega$ is the dynamical component perpendicular to $\boldsymbol{m}_0$. When magnons (spin waves) are excited in the FI, they can be injected into the SC in a process known as the spin pumping effect. The DC interface spin current flowing from the FI into the SC is polarized in the z direction and given by [35]

$$I_z = \sum_{\Omega, \boldsymbol{q}} -2J_{sd}\text{Im}[\tilde{\chi}_{ss}(\Omega, \boldsymbol{q})]m_{\Omega, \boldsymbol{q}}^2, \tag{1}$$

where J_{sd} is the exchange coupling strength and m_Ω is the Fourier amplitude of $\boldsymbol{m}_\Omega$. $\tilde{\chi}_{ss}(\Omega, \boldsymbol{q})$ is the total dynamical spin susceptibility $\tilde{\chi}_{ss}(\Omega, \boldsymbol{q}) = S_+(\Omega, \boldsymbol{q})/h_+(\Omega, \boldsymbol{q})$, where S is the dynamical spin of the SC, h is the proximity-induced exchange field $\boldsymbol{h} = J_{sd}\boldsymbol{m}/d$ [36], and for a vector $A = (A_x, A_y, A_z)$ the $\pm$ component is defined as $A_\pm = A_x \pm iA_y$. One can see that for a fixed J_{sd}, the efficiency of the magnon injection is solely determined by $\tilde{\chi}_{ss}(\Omega, \boldsymbol{q})$. The spin susceptibility of superconductors has been extensively studied [30,37–39]. However, the previous theories, based on the static mean-field description, failed to explain the peak of the iSHE signal observed in the spin Seebeck experiment [34]. In this work, we start with the general partition function of the SC, $Z = \int D[\bar{\Psi}, \Psi, \bar{\Delta}, \Delta]e^{-S}$ obtained by performing the Hubbard-Stratonovich transformation. The action S is given by

$$\begin{aligned} S = \ &\beta \sum_{K, Q} \bar{\Psi}_K(-i\omega + \epsilon_{\tilde{k}} - \boldsymbol{h} \cdot \boldsymbol{\sigma})\Psi_K + \Delta_Q \Psi_{K+Q}\Psi_{-K} \\ &+ \bar{\Delta}_{-Q}\bar{\Psi}_K\bar{\Psi}_{-K-Q} + \frac{\bar{\Delta}_{-Q}\Delta_Q}{U}. \end{aligned} \tag{2}$$

Here $K = (\omega, \boldsymbol{k})$ and $Q = (\Omega, \boldsymbol{q})$ are the four-momenta of the electrons and magnons, and $\omega = (2n + 1)\pi T$ and $\Omega = 2n\pi T$ are the Matsubara frequencies with $n \in Z$ and $\beta = 1/T$. $\epsilon_{\tilde{k}}$ is the energy dispersion of the electron in the normal state and $\tilde{\boldsymbol{k}}$ is the covariant derivative $\tilde{\boldsymbol{k}} = \boldsymbol{k} + \alpha[\sigma_y, -\sigma_x, 0]$, where α is the spin-orbit coupling strength. $\boldsymbol{h}$ is the proximity-induced exchange field, and U is the BCS interaction. Here we only consider the on-site interaction so that no triplet pairing is

generated. In the mean-field theory, one can ignore the path integral over Δ and replace it by its saddle-point value Δ_0 which is determined by the minimization of the action $\frac{\partial S}{\partial \Delta}|_{\Delta = \Delta_0} = 0$ after integrating out the fermion fields.

To include the Higgs mode, we go beyond the mean-field theory and write the order parameter as $\Delta = \Delta_0 + \eta$, where η is the deviation of Δ from its saddle-point value Δ_0. Here we only consider the amplitude fluctuation of Δ, so η is real. Expanding the action to the second order in η and the strength of the external Zeeman field $h_\pm$ gives $S = S_0 - S_2$ with [40]

$$S_2 = \beta \sum_Q [\eta(-Q) \quad h_-(-Q)] \begin{bmatrix} -\chi_{\Delta\Delta}^{-1} & \chi_{\Delta s} \\ \chi_{s\Delta} & \chi_{ss} \end{bmatrix} \begin{bmatrix} \eta(Q) \\ h_+(Q) \end{bmatrix}. \tag{3}$$

Here, all the susceptibilities are functions of Q. S_0 is the mean-field action without the external field. In usual superconductors the off-diagonal susceptibilities $\chi_{\Delta s}$ and $\chi_{s\Delta}$ vanish as required by the time-reversal symmetry and the (spin) rotation symmetry because these operations change the sign of h_+ but have no effect on η [41,42]. In the system under consideration, the proximity-induced static exchange field breaks the time-reversal symmetry and Rashba spin-orbit coupling (RSOC) breaks the (spin) rotation symmetry. Thus the pair-spin susceptibility does not have to vanish, allowing for a nonzero Higgs-spin coupling.

Then it is straightforward to calculate the total spin susceptibility $\tilde{\chi}_{ss}$ by integrating out the η field

$$\tilde{\chi}_{ss} = \chi_{ss} - \chi_{s\Delta}\chi_{\Delta\Delta}\chi_{\Delta s}. \tag{4}$$

The imaginary part of $\chi_{\Delta\Delta}$ is sharply peaked at the Higgs frequency $\Omega = 2\Delta$ dramatically modifying the total spin susceptibility.

II. PHENOMENOLOGICAL THEORY

Before we go into the detailed calculations, we use a simple phenomenological theory to illustrate the effect of RSOC. It has been shown that RSOC can induce a Dzyaloshinskii-Moriya (DM) interaction in superconductors described by the DM free energy [43]

$$F_{DM} = \sum_i \int d\boldsymbol{r}|\Delta|^2 \boldsymbol{d}_{\alpha,i} \cdot (\boldsymbol{h} \times \nabla_i \boldsymbol{h}), \tag{5}$$

where both $\Delta = \Delta(\boldsymbol{r})$ and $\boldsymbol{h} = \boldsymbol{h}(\boldsymbol{r})$ are position dependent. $\boldsymbol{d}_{\alpha,i}$ is the DM vector proportional to the strength of spin-orbit coupling α. For RSOC $\boldsymbol{d}_\alpha \propto \alpha[\sigma_x, -\sigma_z]$, where α is the spin-orbit coupling strength and σ is the Pauli matrix acting on the spin space. To find the pair spin susceptibility we write $\Delta = \Delta_0 + \eta(t)$, $\boldsymbol{h} = h_0\hat{z} + h_+(t)(\hat{x} + i\hat{y})$, where $\hat{n}$ is the unit vector in the n direction with $n = x, y, z$, and generalize the DM free energy to the time-dependent DM action. Here we consider the case where the spin wave is propagating in the z direction $h_+(t, \boldsymbol{r}) = \sum_{\Omega, q_z} h_+(\hat{x} + i\hat{y})e^{i(\Omega t - q_z z)}$. Focusing on the first-order terms in $\eta(t)$ and $h_+(t)$ and Fourier transforming them to momentum and frequency space, the DM action can be written as

$$S_{DM1} = \beta \sum_{\Omega, q_z} iq_z\Delta_0 h_0 h_+(\Omega, q_z)\eta(\Omega, q_z)\tilde{\boldsymbol{d}}_{\alpha,z}(\Omega, q_z)(i\hat{x} - \hat{y}),$$

$$\tag{6}$$

where $\tilde{d}_{\alpha,i}$ is the dynamical DM vector, which has the same finiteness and spin structure as $d_{\alpha,i}$ from symmetry analysis. From the above expression, one can see that the Higgs mode couples linearly with the spin degree of freedom in the presence of RSOC.

III. SPIN SUSCEPTIBILITY

We adopt the quasiclassical approximation to systematically evaluate the susceptibilities. In the diffusive limit, this system can be described by the Usadel equation [19,37,44–48]

$$-i\{\tau_3 \partial_t, \hat{g}\} = D\tilde{\nabla}(\hat{g}\tilde{\nabla}\hat{g}) - i[H_0, \hat{g}] + [Xe^{i(\Omega t - q_z z)}, \hat{g}]. \quad (7)$$

Here $\hat{g}$ is the quasiclassical Green's function, $D = v_F \tau^2/3$ is the diffusion constant, and τ is the disorder scattering time. $H_0 = -ih_0 \sigma_3 + \Delta_0 \tau_1$, where h_0 is the proximity-induced effective static exchange field and τ_i is the Pauli matrix acting on the particle-hole space. $\tilde{\nabla} = (\tilde{\nabla}_z, \tilde{\nabla}_x)$ is the covariant derivative defined by $\tilde{\nabla}_z \cdot = \nabla_z + i\alpha[\sigma_x, \cdot]$, $\tilde{\nabla}_x \cdot = \nabla_x - i\alpha[\sigma_z, \cdot]$. The Usadel equation is supplemented by the normalization condition $\hat{g}^2 = 1$. In the quasiclassical approximation the approximate particle-hole (PH) symmetry of the full Hamiltonian becomes exact. In the linear response theory, the external oscillating field X is small and can be treated as a perturbation. Thus we can write the quasiclassical Green's function as $\hat{g} = \hat{g}_0 e^{i\omega(t_1 - t_2)} + \hat{g}_X e^{i(\omega+\Omega)t_1 - i\omega t_2 - iq_z z}$, where $\hat{g}_0$ is the static Green's function and $\hat{g}_X$ is the perturbation of the Green's function describing the response to the external field. Solving the Usadel equation we obtain the quasiclassical Green's function, the anomalous's Green function $F = N_e \text{Tr}[\tau_1 \hat{g}]/4i$, and the σ_+ component of spin in the SC $\langle s \rangle = N_e \text{Tr}[\sigma_- \tau_3 \hat{g}]/4i$, where N_e is the electron density of states at the Fermi surface and Tr is the trace. The susceptibilities can be evaluated as

$$\hat{\chi} = \begin{bmatrix} \chi_{\Delta\Delta}^{-1} & \chi_{\Delta s} \\ \chi_{s\Delta} & \chi_{ss} \end{bmatrix} = \begin{bmatrix} \frac{\partial F}{\partial \eta} + \frac{1}{U} & \frac{\partial F}{\partial h_+} \\ \frac{\partial \langle s \rangle}{\partial \eta} & \frac{\partial \langle s \rangle}{\partial h_+} \end{bmatrix}. \quad (8)$$

Let us first set $X = \Delta' \tau_1$ and consider the pair susceptibility. We assume the RSOC is weak and treat α as a perturbation. At $q = 0$ and zeroth order in α, we have

$$\chi_{\Delta\Delta}(i\Omega) = \left[\frac{N_e T}{2} \sum_{\omega,\sigma} \frac{4\Delta^2 + \Omega^2}{s_\sigma(\omega)(4\omega^2 - \Omega^2)} \right]^{-1}, \quad (9)$$

where $s_\sigma(\omega) = \sqrt{(\omega + i\sigma h)^2 + \Delta^2}$, with $\sigma = \pm 1$. To get the pair susceptibility as a function of real frequency, we need to perform an analytical continuation [41]. Thus $i\Omega$ is replaced by $\Omega + i0^+$. One can see that the $\chi_{\Delta\Delta}$ is peaked at the Higgs frequency $\Omega = 2\Delta$.

We numerically calculate $\chi_{\Delta\Delta}$ with finite momentum and show the results in Fig. 2 [41,49]. One can see that the imaginary part of the inverse of the pair susceptibility exhibits a sharp peak when the driving frequency equals $2\Delta_0$. With a finite momentum, the Higgs mode is damped in the sense that the peak in the Higgs spectrum has a finite height and width.

To study the response of this system to the external exchange field we set $X = h_+ \sigma_+ \tau_3$. Again we treat α as a
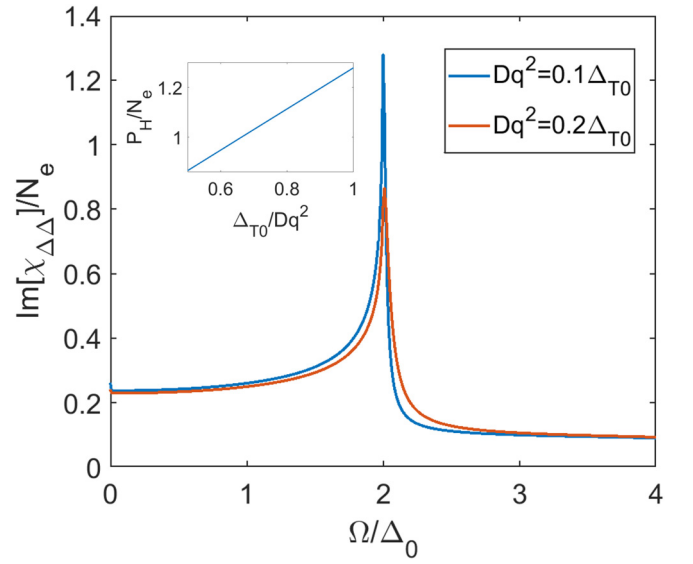

FIG. 2. Imaginary part of the pair susceptibility. This can be interpreted as the spectral weight of the Higgs mode. A significant peak emerges when the driving frequency matches the Higgs frequency $\Omega = 2\Delta_0$. The inset shows the height of the Higgs peak P_H as a function of the inverse of the momentum q. Parameters: $\Delta_0 = 0.8\Delta_{T0}$, $h_0 = 0.5\Delta_{T0}$ with $\Delta_{T0} \equiv \Delta_0(T = 0)$.

perturbation and write the Green's function as

$$\hat{g} = \hat{g}_0 e^{i\omega(t_1 - t_2)} + (\hat{g}_{h0} + \hat{g}_{h\alpha})e^{i(\omega+\Omega)t_1 - i\omega t_2 - iq_z z}, \quad (10)$$

where $\hat{g}_{h0}$ is zeroth order in α and $\hat{g}_{h\alpha}$ is first order in α. The zeroth-order solution in α is given by [41]

$$\hat{g}_{h0} = \hat{g}_{h00} \otimes \sigma_+ = \frac{i[\tau_3 - \hat{g}_\uparrow(1)\tau_3 \hat{g}_\downarrow(2)]h_\Omega \sigma_+}{s_\uparrow(1) + s_\downarrow(2)}, \quad (11)$$

where $\hat{g}_{\uparrow/\downarrow} = \frac{(\omega \pm ih_0)\tau_3 + \Delta\tau_1}{s_{\uparrow/\downarrow}}$ and $s_{\uparrow/\downarrow} = \sqrt{(\omega \pm ih_0)^2 + \Delta^2}$. $\hat{g}_{h00}$ is a 2×2 matrix in the particle-hole space. Without doing detailed calculations, one can immediately see that $\chi_{\Delta s}$ has to vanish without RSOC because $\hat{g}_h$ has no σ_0 component. In this case the external exchange field cannot activate the Higgs mode. To get a finite pair-spin susceptibility we need to consider the first-order terms in α which break the spin rotation symmetry. The first-order solution in α yields $\hat{g}_{h\alpha} = \text{diag}(\hat{g}_{h\alpha\uparrow}, \hat{g}_{h\alpha\downarrow})$ with

$$\hat{g}_{h\alpha\uparrow/\downarrow} = 2iD\alpha \frac{\hat{g}_{0\uparrow/\downarrow}[\hat{g}_{h00}, \hat{g}_{0\uparrow/\downarrow}]}{s_{\uparrow/\downarrow}(\omega_1) + s_{\uparrow/\downarrow}(\omega_2)}. \quad (12)$$

Since the zeroth-order term does not contribute to the pair-spin susceptibility, we have $\chi_{\Delta s} = \text{Tr}[\tau_1 \hat{g}_{h\alpha}]/4ih_+$. We compare this analytical result with the nonperturbative numerical solution of the Usadel equation in Fig. 3. It shows that the perturbative approach is accurate at high temperatures when $D\alpha^2 \ll \Delta_0, T$, and captures the qualitative behavior of $\chi_{\Delta s}$ also at the low temperatures. Another feature of this pair-spin susceptibility is that at a lower frequency ($\Omega = 0.8\Delta_{T0}$), $\chi_{\Delta s}$ is suppressed at low temperatures because the spin excitation is frozen by the pair gap at low temperatures. On the other hand, at higher frequency ($\Omega = \Delta_{T0}$), $\chi_{\Delta s}$ is slightly enhanced at low temperatures.
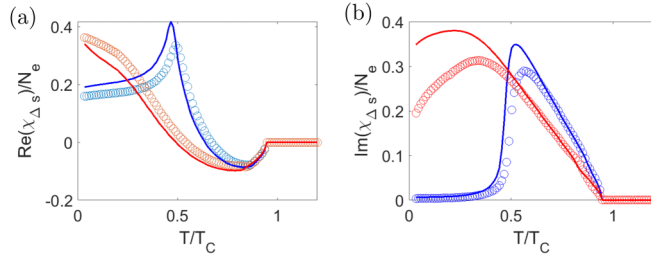
FIG. 3. Real part (a) and imaginary part (b) of pair-spin susceptibility. The solid line is the approximate result calculated from Eq. (12) and the circles show the numerical solution from Eq. (7). Parameters used here are $\Omega = 0.8\Delta_{T0}$ for the blue lines, $\Omega = \Delta_{T0}$ for the red lines, $h_0 = 0.5\Delta_{T0}$, and $Dq_z^2 = D\alpha^2 = 0.01\Delta_{T0}$.

We can also get the bare spin susceptibility from $\hat{g}_{h0}$, $\chi_{ss} = \text{Tr}[\sigma_-\tau_3\hat{g}_{h0}]/4ih_+$. Then it is straightforward to calculate the total spin susceptibility according to Eq. (4). The results are shown in Fig. 4. The total spin susceptibility exhibits a significant peak near critical temperature. This is a signature of the Higgs mode with the frequency $\Omega = 2\Delta_0$. The dependence of the total susceptibility on the strength of RSOC is studied in the Supplemental Material [41]. The details depend sensitively on the amount of disorder, as in the disordered case increasing RSOC leads to a stronger spin relaxation. We note that even though the pair-spin susceptibility is linear in momentum q_z, the magnon momentum need not be large for the detection of the Higgs mode. This is because the spectral weight of the Higgs mode is proportional to $1/q_z^2$ at the Higgs frequency, so that the height of the peak in the total spin susceptibility is independent of the magnon momentum.
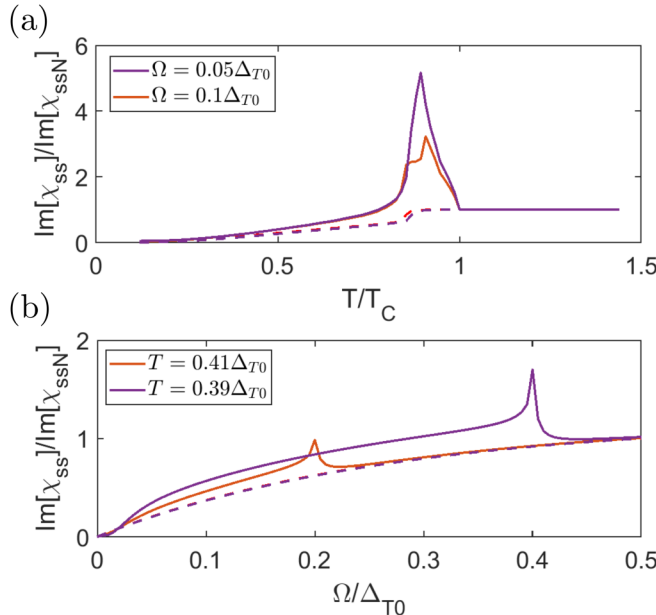

FIG. 4. (a) Total spin susceptibility as a function of temperature with a fixed frequency. (b) Total spin susceptibility as a function of frequency with a fixed temperature. The dashed lines are the spin susceptibilities without the effect of the Higgs mode. The two temperatures have been chosen so that $\Delta(T_1) = 0.2\Delta_{T0}$ and $\Delta(T_2) = 0.1\Delta_{T0}$. The Higgs peak thus shows up when $\Omega = 2\Delta(T)$. The parameters used here are $h_0 = 0.5\Delta_{T0}$ and $Dq_z^2 = D\alpha^2 = 0.01\Delta_{T0}$.

IV. EXPERIMENTAL DETECTION

We propose that the Higgs mode in Rashba superconductors can be detected in the spin pumping experiment as shown in Fig. 1. Magnons in the FI with momentum $\boldsymbol{q}$ and frequency Ω are injected from one side of FI and propagate in the z direction towards the other end. Due to the spin pumping effect, part of the magnons can be absorbed by the SC on top of it and converted to quasiparticles. This spin injection causes a spin current I_s flowing in the out-of-plane direction. In the presence of RSOC, I_s is converted into a charge current I_e via the iSHE $I_e = \theta_{xz}^z I_s$, where θ is the spin Hall angle [50]. When the width of the SC is smaller than the charge imbalance length the nonequilibrium charge accumulation cannot be totally relaxed resulting in a finite resistance ρ of the SC. Therefore a voltage can be measured across the SC, given by

$$V = \theta_{xz}^z \rho \sum_{\Omega,\boldsymbol{q}} -2J_{sd}\text{Im}[\tilde{\chi}_{ss}(\Omega, \boldsymbol{q})]m_\Omega^2. \quad (13)$$

Thus by tuning the temperature or the frequency of magnon, one can observe a peak in the voltage [34]. Meanwhile we can also obtain the magnon absorption rate defined as the energy of the absorbed magnons divided by time

$$W = 2\Omega \sum_{\Omega,\boldsymbol{q}} -2J_{sd}\text{Im}[\tilde{\chi}_{ss}(\Omega, \boldsymbol{q})]m_\Omega^2. \quad (14)$$

This magnon absorption rate results in a dip in the magnon transmission rate which is experimentally measurable.

V. CONCLUSION

In this paper, we consider a FI/SC bilayer with RSOC in the bulk of the SC. Using symmetry arguments and microscopic theory, we show that the Higgs mode in the SC couples linearly with an external exchange field. This Higgs-spin coupling hugely enhances the total spin susceptibility near a critical phase transition point, which can be detected using iSHE or via strong frequency-dependent changes in the magnon transmission. Note that in this work, we consider the diffusive limit where the disorder strength is stronger than the RSOC and exchange field. However, our conclusion on Higgsspin coupling should still be valid in the case of strong RSOC. In fact, we expect that the coupling is much stronger with strong SOC in the clean limit. In the diffusive limit, the RSOC together with disorder effectively generate spin relaxation which reduces the proximity-induced exchange field suppressing the Higgs-spin coupling. On the other hand, in the clean case without disorder this effect is absent and hence the Higgs-spin coupling can be stronger. We also compare the Higgs mode in the diffusive limit and ballistic limit in the Supplemental Material [41].

[1] N. Bittner, D. Einzel, L. Klam, and D. Manske, Phys. Rev. Lett. **115**, 227002 (2015).

[2] P. W. Anderson, Phys. Rev. **130**, 439 (1963).

[3] P. W. Higgs, Phys. Rev. Lett. **13**, 508 (1964).

[4] I. Kulik, O. Entin-Wohlman, and R. Orbach, J. Low Temp. Phys. **43**, 591 (1981).

[5] A. Pashkin and A. Leitenstorfer, Science **345**, 1121 (2014).

[6] P. B. Littlewood and C. M. Varma, Phys. Rev. B **26**, 4883 (1982).

[7] P. B. Littlewood and C. M. Varma, Phys. Rev. Lett. **47**, 811 (1981).

[8] M.-A. Méasson, Y. Gallais, M. Cazayous, B. Clair, P. Rodiere, L. Cario, and A. Sacuto, Phys. Rev. B **89**, 060503(R) (2014).

[9] R. Grasset, Y. Gallais, A. Sacuto, M. Cazayous, S. Mañas-Valero, E. Coronado, and M.-A. Méasson, Phys. Rev. Lett. **122**, 127001 (2019).

[10] R. Grasset, T. Cea, Y. Gallais, M. Cazayous, A. Sacuto, L. Cario, L. Benfatto, and M.-A. Méasson, Phys. Rev. B **97**, 094502 (2018).

[11] T. Cea and L. Benfatto, Phys. Rev. B **90**, 224515 (2014).

[12] D. N. Basov, R. D. Averitt, D. vanderMarel, M. Dressel, and K. Haule, Rev. Mod. Phys. **83**, 471 (2011).

[13] R. Matsunaga, Y. I. Hamada, K. Makise, Y. Uzawa, H. Terai, Z. Wang, and R. Shimano, Phys. Rev. Lett. **111**, 057002 (2013).

[14] R. Matsunaga, N. Tsuji, H. Fujita, A. Sugioka, K. Makise, Y. Uzawa, H. Terai, Z. Wang, H. Aoki, and R. Shimano, Science **345**, 1145 (2014).

[15] M. Beck, I. Rousseau, M. Klammer, P. Leiderer, M. Mittendorff, S. Winnerl, M. Helm, G. N. Gol'tsman, and J. Demsar, Phys. Rev. Lett. **110**, 267003 (2013).

[16] M. Silaev, Phys. Rev. B **99**, 224511 (2019).

[17] M. A. Silaev, R. Ojajärvi, and T. T. Heikkilä, Phys. Rev. Research **2**, 033416 (2020).

[18] R. Shimano and N. Tsuji, Annu. Rev. Condens. Matter Phys. **11**, 103 (2020).

[19] A. Moor, A. F. Volkov, and K. B. Efetov, Phys. Rev. Lett. **118**, 047001 (2017).

[20] S. Nakamura, Y. Iida, Y. Murotani, R. Matsunaga, H. Terai, and R. Shimano, Phys. Rev. Lett. **122**, 257001 (2019).

[21] S. Nakamura, K. Katsumi, H. Terai, and R. Shimano, Phys. Rev. Lett. **125**, 097004 (2020).

[22] M. Puviani, L. Schwarz, X.-X. Zhang, S. Kaiser, and D. Manske, Phys. Rev. B **101**, 220507(R) (2020).

[23] Z. M. Raines, A. A. Allocca, M. Hafezi, and V. M. Galitski, Phys. Rev. Research **2**, 013143 (2020).

[24] I. Žutić, J. Fabian, and S. Das Sarma, Rev. Mod. Phys. **76**, 323 (2004).

[25] J. Linder and J. W. Robinson, Nat. Phys. **11**, 307 (2015).

[26] Y. Tserkovnyak, A. Brataas, and G. E. W. Bauer, Phys. Rev. Lett. **88**, 117601 (2002).

[27] E. Saitoh, M. Ueda, H. Miyajima, and G. Tatara, Appl. Phys. Lett. **88**, 182509 (2006).

[28] K. Ando, S. Takahashi, J. Ieda, Y. Kajiwara, H. Nakayama, T. Yoshino, K. Harii, Y. Fujikawa, M. Matsuo, S. Maekawa *et al.*, J. Appl. Phys. **109**, 103913 (2011).

[29] Y. Tserkovnyak, A. Brataas, and G. E. W. Bauer, Phys. Rev. B **66**, 224403 (2002).

[30] T. Kato, Y. Ohnuma, M. Matsuo, J. Rech, T. Jonckheere, and T. Martin, Phys. Rev. B **99**, 144411 (2019).

[31] S. Takahashi and S. Maekawa, Phys. Rev. Lett. **88**, 116601 (2002).

[32] S. Takahashi and S. Maekawa, Sci. Technol. Adv. Mater. **9**, 014105 (2008).

[33] T. Wakamura, H. Akaike, Y. Omori, Y. Niimi, S. Takahashi, A. Fujimaki, S. Maekawa, and Y. Otani, Nat. Mater. **14**, 675 (2015).

[34] K.-R. Jeon, J.-C. Jeon, X. Zhou, A. Migliorini, J. Yoon, and S. S. Parkin, ACS Nano **14**, 15874 (2020).

[35] R. Ojajärvi, T. T. Heikkilä, P. Virtanen, and M. A. Silaev, Phys. Rev. B **103**, 224524 (2021).

[36] T. T. Heikkilä, M. A. Silaev, P. Virtanen, and F. S. Bergeret, Prog. Surf. Sci. **94**, 100540 (2019).

[37] M. A. Silaev, Phys. Rev. B **102**, 144521 (2020).

[38] K. V. Samokhin, Phys. Rev. B **103**, 174505 (2021).

[39] P. A. Frigeri, D. F. Agterberg, and M. Sigrist, New J. Phys. **6**, 115 (2004).

[40] T. Cea, C. Castellani, G. Seibold, and L. Benfatto, Phys. Rev. Lett. **115**, 157002 (2015).

[41] See Supplemental Material at http://link.aps.org/supplemental/10.1103/PhysRevB.106.024514 for details of the symmetry operators, derivation of the susceptibilities, which includes Ref. [51].

[42] In general h_+ is inhomogeneous and the gradient of h_+ breaks the mirror symmetry locally. Thus we do not need to consider the mirror symmetry of the SC.

[43] M. A. Silaev, D. Rabinovich, and I. Bobkova, arXiv:2108.08862.

[44] K. D. Usadel, Phys. Rev. Lett. **25**, 507 (1970).

[45] W. Belzig, F. K. Wilhelm, C. Bruder, G. Schön, and A. D. Zaikin, Superlattices Microstruct. **25**, 1251 (1999).

[46] F. S. Bergeret, A. F. Volkov, and K. B. Efetov, Rev. Mod. Phys. **77**, 1321 (2005).

[47] F. S. Bergeret and I. V. Tokatly, Phys. Rev. B **89**, 134517 (2014).

[48] F. S. Bergeret and I. V. Tokatly, Phys. Rev. Lett. **110**, 117003 (2013).

[49] The code used to obtain the results in this paper can be found at https://gitlab.jyu.fi/jyucmt/sssc-higgs-rashba.

[50] I. V. Tokatly, Phys. Rev. B **96**, 060502(R) (2017).

[51] J. Linder and M. Amundsen, Phys. Rev. B **105**, 064506 (2022).